

# The Fretting Fatigue Behavior of Bolted Assemblies

**Ali Benhamena, Laïd Aminallah, Abdelghani Baltach, Abdelkrim Aid, Mohamed Benguediab, Abdelwaheb Amrouche and Nouredine Benseddiq**

**Abstract** This study is a contribution to various scientific researches on fracture behavior of bolted joints. In our study, a three-dimensional finite element model (3D-FEM) is developed to predict the mechanical behavior of bolted joints. Fretting-fatigue tests and numerical simulations were conducted to study the effect of the clamping torque on the fatigue behavior and failure mode of bolted assemblies. The results obtained in numerical simulations are evaluated and compared with experimental results. The numerical model showed the capacity to simulate the behavior of the bolted assemblies under fatigue. Crack initiation changed from the edge of the hole to close the edge of the contact zone. A good correlation was found between the FEM simulations and the experimental results.

---

A. Benhamena (✉) · L. Aminallah · A. Baltach · A. Aid  
Laboratory LPQ3M, University of Mascara, BP 763, Mascara, Algeria  
e-mail: ali\_benhamena@yahoo.fr

L. Aminallah  
e-mail: abdaminn@yahoo.fr

A. Baltach  
e-mail: baltachabdelghani@yahoo.fr

A. Aid  
e-mail: aid\_abdelkrim@yahoo.com

A. Benhamena · L. Aminallah · A. Aid · N. Benseddiq  
Laboratory of Mechanic of Lille, University of Science and Technology of Lille,  
UMR CNRS, 8107 USTL, France  
e-mail: noureddine.benseddiq@univ-lille1.fr

M. Benguediab  
Department of Mechanical engineering, University of Sidi Bel Abbes,  
BP 89, Cité Ben M'hidi, 22000 Sidi Bel Abbes, Algeria  
e-mail: benguediab\_m@yahoo.fr

A. Amrouche  
Laboratoire de Génie Civil et géo-Environnement LGCgE, EA4515, Université d'Artois,  
Faculté des Sciences Appliquées Béthune, Béthune, France  
e-mail: abdelwaheb.amrouche@univ-artois.fr

**Keywords** Clamping force · Torque · Fretting fatigue · Crack initiation site · Stick · Slip · Adhesion

## 1 Introduction

Fretting damage is considered an important failure mechanism for a variety of mechanical components and assemblies. However, the analysis of practical fretting problems entails significant difficulties related to the characterization of the contact interactions [1–5]. Bolted joints in mechanical structures transmit a more important effort in various applications. According to Valtinat et al. [6] bolted joints have higher tensile and fatigue strengths than welded joints. The prediction of fracture and the reliability of such assembly in various practical applications are primordial given their impact on the economic plan and security. Fretting is caused by the oscillating movement with small amplitude that may occur between contacting surfaces subjected to vibration. The oscillations cause sliding to occur in a small region at the edge of contact, while the center of contact remains stuck together. The damage is related to cyclic loading and relative displacement at the interface in such assemblies. The amplitude of relative displacement (slip) and the contact forces (or contact pressure) are two significant factors, which control the fretting fatigue behavior. Lee and Mall [7] investigated the variation of fretting fatigue life with the increase of amplitude of relative displacement on Ti-6Al-4V material. They postulated that the amplitude of relative displacement increases from 0 to 50  $\mu\text{m}$  (partial slip and mixed slip), the fretting fatigue life decreases. On the other hand, the increase of relative displacement from 50 to more than 100  $\mu\text{m}$  (gross slip), induces the increase of fretting fatigue life. In the same context, several studies [8–11] have been carried out to investigate the damage of contact surface and the effect of fastening forces. All these authors observe that the fretting fatigue life decreases with the increase of contact forces. It is well known that stress distribution at the contact edge (i.e. the tangential stress and the compressive stress) plays a dominant role in influencing fretting fatigue strength [12–14]. From this point of view, in the previous study, a fretting fatigue strength prediction method based on the tangential stress range compressive stress range diagram has been developed and discussed for Ni-Cr-Mo-V steel [15]. Chakherlou et al. [16] conducted fatigue tests and numerical simulation to study the effect of cold expansion and bolt clamping on fretting fatigue behaviour of Al 2024-T3 in double shear lap joints. The results reveal that significant changes on the fatigue behaviour of the double shear lap joints at different load ranges. Depending on the degree of cold expansion and clamping torque. The references cited above show some contradictory tendencies of the fretting fatigue life. In service and under cyclic loading, the relative displacement at the interface is inevitable for bolted assemblies, in addition the effect of clamping force on the stress concentration close to the hole, the frictional stresses and the friction coefficient are not fully understood

and represent a very active research field. This fact has led the authors to focus on the current study, in order to contribute in this way. We recall also, that the present study is an extension of previous studies [2]. Finite element analysis (FEA) is an important tool to design a practical mechanical component, such as, for example, pipelines. The three-dimensional finite element method 3D-FEM under consideration of non-linear models can predict well the behaviour of bolted assemblies (steel-aluminium) loaded in fatigue. Moreover, a number of the fatigue–fractured sections of the specimens are studied to help identify the location of crack initiation and also to examine the propagation regions.

## 2 Experimental and Numerical Model

### 2.1 Materials and Specimens

The details of the experimental fretting-fatigue test programme were previously reported in [2] and are just briefly explained here. Aluminium alloy A6xxxx from 6.0 mm thickness and high strength low alloy steel (HSLA355) of 3.0 mm thickness were used to produce (6.0 mm A6xxxx + 3.0 mm HSLA355) joints for this investigation (Fig. 1) and the fretting fatigue test method is shown in Fig. 2, full details of the test setup are given elsewhere [1, 2].

### 2.2 Finite Element Model

Fretting tests may be carried out in the partial slip regime. As highlighted by Hills et al. [17], it is very difficult to achieve a well controlled experiment using an external actuator due to the low displacement amplitudes. Although the relative displacement cannot be easily measured and its value is required, an analysis of the stress field at the process zone (contact zone) in partial slip regime. Finite element analysis (FEA) is an important tool to design practical mechanical joints, such as bolted assemblies. According to the dimensions of the structure, a three-dimensional model was generated using the commercial software ANSYS<sup>®</sup> (ANSYS 11 [18]) in order to determine and to perform the analyses of the stress field at the contact zone. The bolted assembly shown in Fig. 2 is symmetric in the longitudinal direction (y-direction). So, a half model with symmetry conditions was used in the finite element model in order to reduce the calculation time (Fig. 2a). Three-dimensional brick elements (SOLID45) are used for modelling of the bolted assembly. This element is defined by eight nodes and each having three degrees of freedom. In addition, a surface-to-surface contact element, which consists of contact elements (CONTAC173) and target surface elements (TARGE169), is used on the interfaces between all connected parts of the bolted assembly in order to

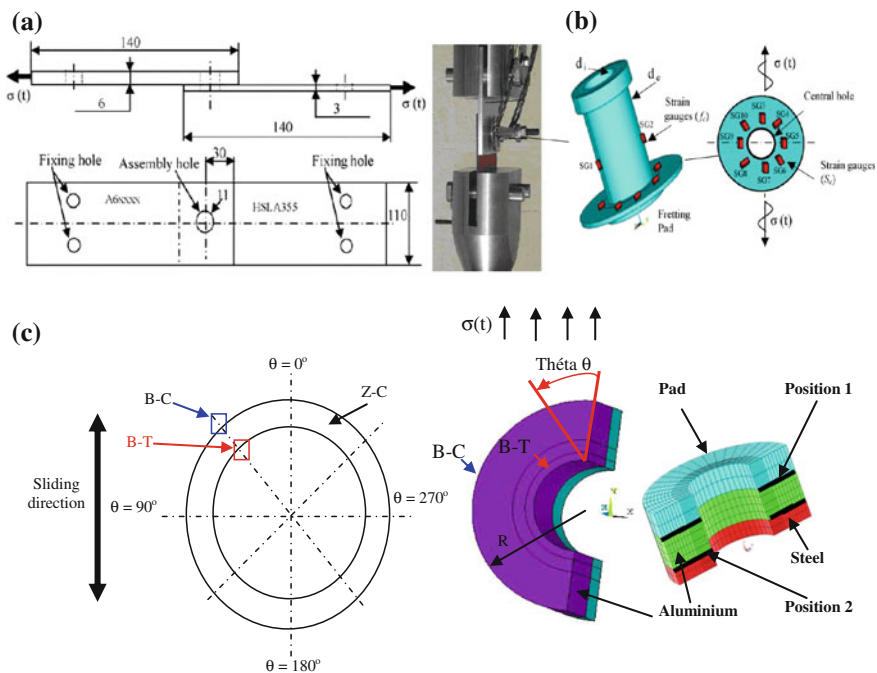


**Fig. 1** a Specimen geometry (all dimensions in mm), b schematic drawing of central part of the specimen used in fretting fatigue tests and the strain gauges and c nomination of the Cartesian coordinates, different planes and positive  $\theta$  direction at a half of bolted assemblies

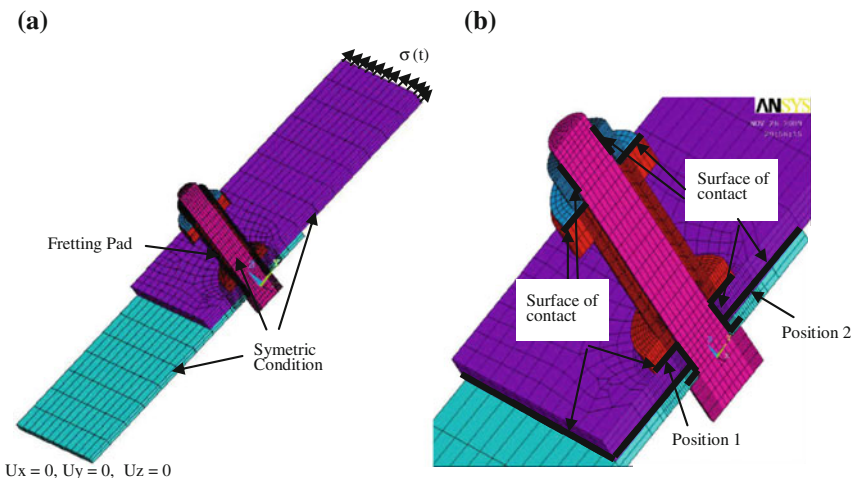


**Fig. 2** a Geometrical and finite-element mesh of assembly, b modeling of contact surface (damaged surface: position 1 and position 2)

simulate numerically the contact problems. Friction between the contact surfaces at the connection is modeled using the classical Coulomb model, where the friction coefficient was set at 0.2. Various mesh schemes are tried to achieve convergence. The optimized model has 14,752 nodes, 17,020 elements and 190 contact elements. A two-step nonlinear analysis was performed in order to simulate the clamping force numerically, in the first step, the preload (clamping force) was modelled as a uniform negative pressure applied on the screw and a positive pressure applied over a ring of 10 mm inner radius and 16 mm outer radius, this ring represents the action of the nut (Fig. 2b). This phase represents the joining of the bolted assembly. After this operation, there is a relaxation of the tensile strain due to the deformability of the pad and the plates under the clamping force action, on attaining equilibrium and in the second step, this assembly was subjected to cyclic loading that generated a multi-axial stress fields at the contact zone. The bolt shank had a clearance of 1 mm due to the dimensional tolerance of the boltholes in the two plates (steel and aluminum) and pad. In practice the plates and pad are tightened by a torque applied to the bolts; this action was simulated by transferring the torque as axial strain in the bolt shank during the assembly process. Although during cyclic loading there is a possibility that the two plates or pad surface in boltholes could contact the surfaces of the bolt shank. However, the clearance was considered large enough for this action not to occur in order to simulate the fretting fatigue at position 1 and at position 2. The theory of incremental plasticity is introduced to model the material nonlinearity. The iterative Newton-Raphson method is used as an approach to solve nonlinear equations by finite elements.

### 3 Results and Discussions

#### 3.1 Validation of the Finite Element Model

The finite element model is validated on the basis of the compressive axial strain measured by the strain gauges (SG1, SG2) glued at the pad during the fretting fatigue test. After that, the numerical model is applied to evaluate the stress distributions at the contact surface in bolted assemblies for various loading condition. Figure 3 shows the compressive axial strain during the simulation of fretting fatigue test under maximal cyclic loading equal to 70 MPa and a tightening torque value of 6 daN.m. We noticed in this case that the compressive strain is strongly concentrated at the interface between the pad and the aluminium plate. This phenomenon can be explained by the fact of strain incompatibility at the interface (position 1, see Fig. 1) and the frictional coefficient effect. Indeed, under this condition and in position at the pad, the compressive strain measured by the strain gauges (SG1, SG2) is 0.001085. At the same position, the compressive strain is calculated numerically and its value equal to 0.000954. So it can be seen according to Fig. 3 that the numerical results of the computational model are in good agreement with experimental results.

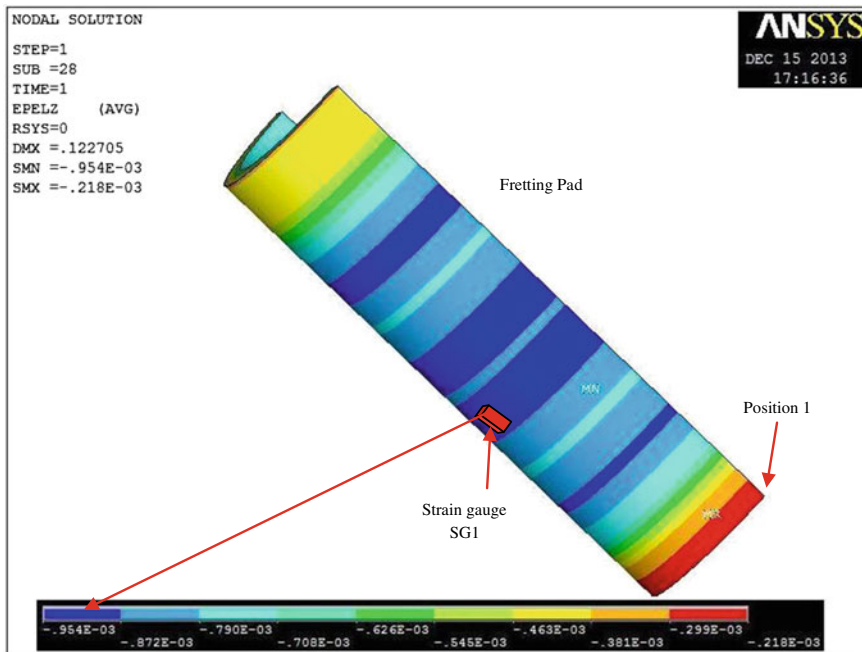


**Fig. 3** Compressive strain at the pad under maximal cyclic loading  $F_{\max} = 12$  KN and torque 6 daN.m

These results were confirmed by the compressive strain (experimental and the numerical results) versus tightening torque presented in Fig. 4; this presents the clamping force variation according to the tightening torque. In this figure we observe that a linear trend was found between the compressive strains measured on the pad as a function of torque (clamped force). This confirms that the material of the pad remains in the elastic region, even for very high compression forces (contact force higher). We note also a fairly good agreement between the numerical and experimental results, this later establishing the confidence in the results of the finite element modeling for bolted assemblies.

### 3.2 Numerical Results and Analysis

Figure 5 shows the stress distribution along the longitudinal direction of cyclic loading ( $\sigma_y$ ) for this loading condition. We observe that the stress distribution is not uniform; this is due to the anti-symmetry of various parameters: the loading conditions, the geometry and the heterogeneity of the behavior of plates. We also observe, on the one hand, that there is a high tensile local stress located at the head of the bolt ( $\sigma_y = 435$  MPa), this is due to the interaction of the stress field

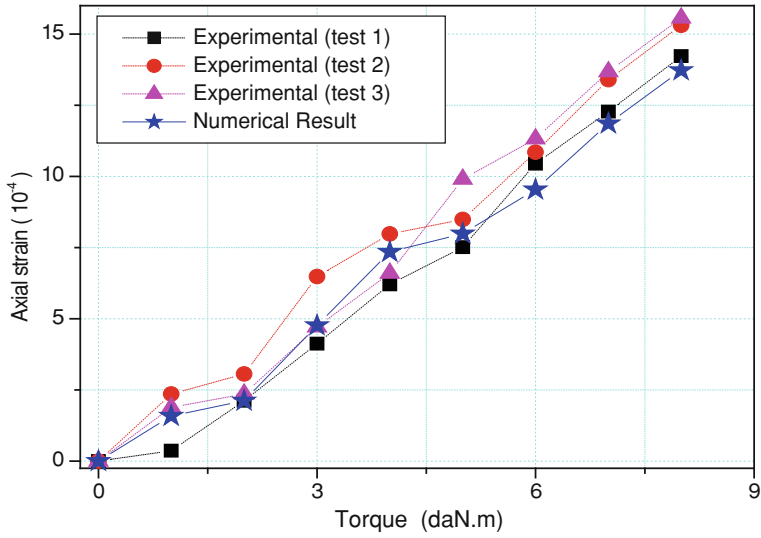


Fig. 4 Axial strain versus tightening torque

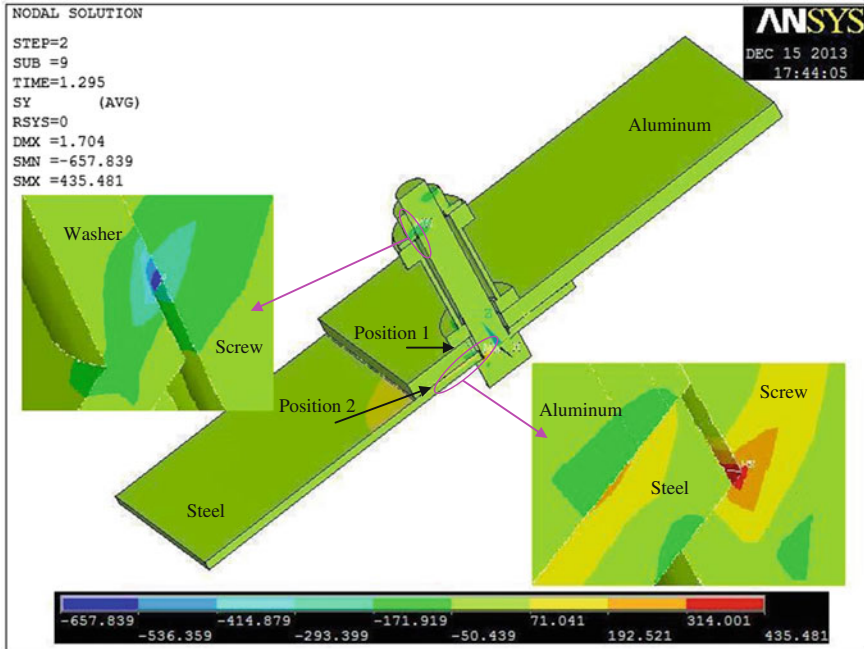
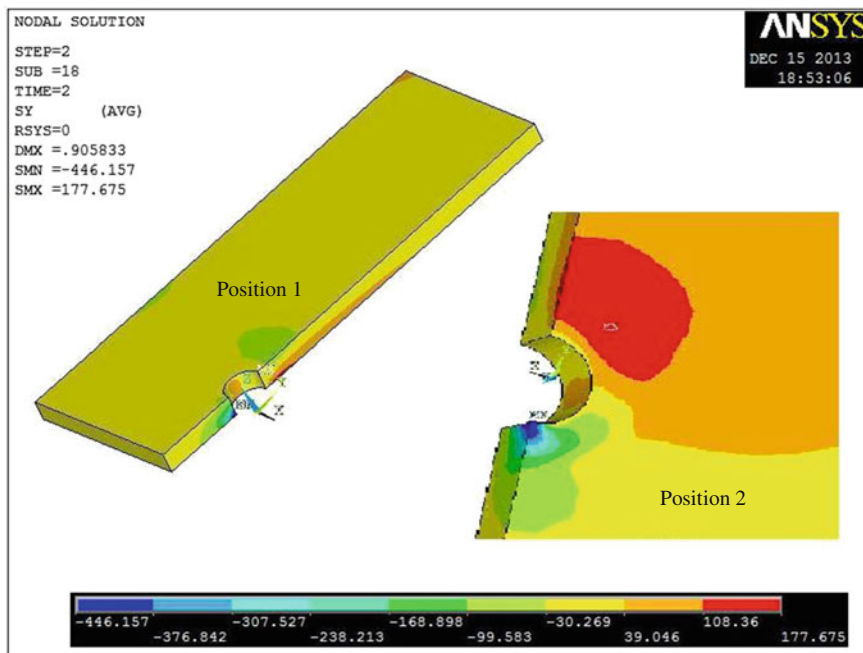


Fig. 5 The distribution of stress  $\sigma_y$  in the direction of cyclic loading of bolted assembly ( $T = 6 \text{ daN.m}$  and  $F_{\max} = 12 \text{ kN}$ )



**Fig. 6** The distribution of stress  $\sigma_y$  in the direction of cyclic loading of aluminium plate ( $T = 6$  daN.m and  $F_{\max} = 12$  KN)

(tension-compression) in the contact surfaces at the interface between the steel plate and the bolt head during sliding. On the other hand, a very high compressive local stress ( $\sigma_y = 657$  MPa) appears in the end of the contact areas between screw and nut. This phenomenon corresponds to a situation that can sometimes appear in such bolted assembly where the field constraint is not homogeneous in threaded elements. These constraints are relatively higher and are located in the screw-nut, which is reasonable when taking into account that these elements (screw and nut) are considered as rigid bodies in the finite element model.

Figure 6 show the distribution of the  $\sigma_y$  stress component in the direction of the cyclic loading for the aluminium plate only. We can see, that the most stressed areas are located in the contact interface near at the connecting element. These areas are located either at the interface between the pad and the aluminium plate (position 1) or at the interface between the steel and aluminium plates (position 2). We observe also a higher compression field located in position 1, while the position 2 is under combined effect (tension and compression effect), the tension is observed at the top of the connecting hole, i.e. at the side were the cyclic loading is applied and the compression is observed at the bottom of the hole.

The explanation for this phenomenon is the following: in the tightening phase, all contact surfaces in the aluminium plate are under compression. After the application of the load (cyclic loading) in direction perpendicular to the plane of



application of the clamping force, a frictional stress is produced at the interface of the contact surfaces, in particular at the interface characterized by the position 2 (interface between the steel and aluminium plates). The presence of a large tensile stress in this position (position 2), leads to the risk of crack initiation in favourable directions at this position (position 2), while the existence of a compressive stress in such position in the contact surface significantly reduces the risk of crack initiation (for example at the near of the hole). We recall that the stress field of the compression and the tension is related by several factors: the coefficient of friction, sliding, sticking, secondary bending effect for this type of bolted assembly, geometrical parameter, etc. According to our experimental results [2] and the observations of Wagle et al. [19] for a bolted assembly under cyclic loading, the level of torque and the amplitude of the cyclic loading are two key variables which control the fretting fatigue life and the wear mechanism in bolted assemblies under fatigue. So, the intensity and the distribution of the stress field at the contact surface determine the risk of failure of bolted assemblies under fatigue.

### 3.2.1 Distribution of Stress at Position 1

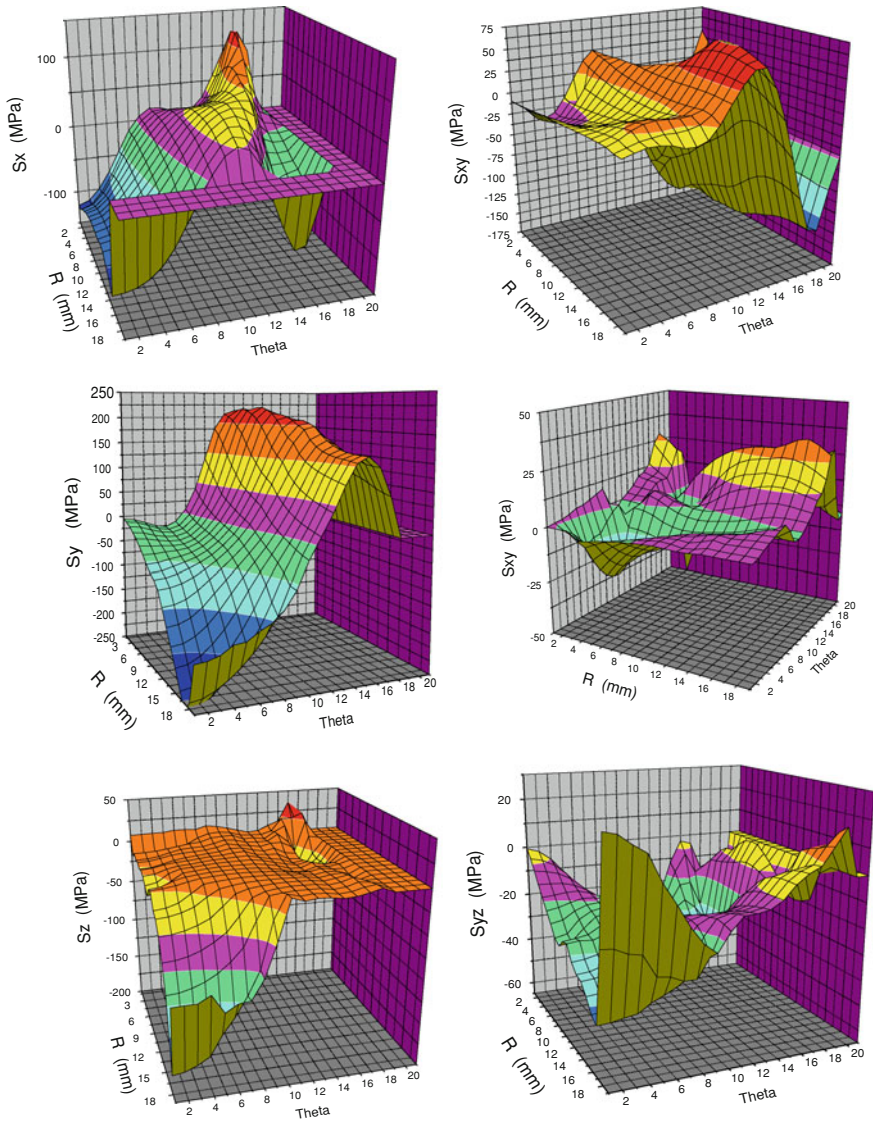
Figure 7 shows the variation of the normal stresses ( $\sigma_x$ ,  $\sigma_y$  and  $\sigma_z$ ) and shear stresses ( $\sigma_{xy}$ ,  $\sigma_{yz}$  and  $\sigma_{xz}$ ) in Cartesian coordinates at the contact surface characterized by the radius  $R$  and angle theta  $\theta$  (see Fig. 1) between aluminum plate and pad (position 1). At the edge of the contact area (BC), for position characterized by the angle  $\theta$  less than  $90^\circ$  ( $\theta < 90^\circ$ ) along the (BC), all the normal stresses ( $\sigma_x$ ,  $\sigma_y$  and  $\sigma_z$ ) are negative values and for position characterized by the angle  $\theta$  greater than  $90^\circ$  ( $\theta > 90^\circ$ ) the two components ( $\sigma_x$  and  $\sigma_y$ ) are positive and the component ( $\sigma_z$ ) is zero. This phenomenon can be explained by the fact that the aluminum plate is under complex loading (tension and compression) along the (BC) contact zone between aluminum plate and pad (position 1). We also observe that the value of shear stress ( $\sigma_{xy}$ ,  $\sigma_{yz}$  and  $\sigma_{xz}$ ) are very low values compared to the value of the normal stresses, therefore the failure mode is governed by the normal stresses. We note that the traction accelerates the risk of cracks in the contact area, while the compression results in the inverse problem. Through a comparison of the stresses evaluated along the edge of the central hole (BT) and the edge of the contact area (BC), we find that the intensity of the stress field in BC is higher than that in BT. Some stress component ( $\sigma_z$ ) has significant negative values at the edge of the hole (BT). This is clearly due to the magnitude of torque which leads to produce an intense compressive stress field at the edge of the hole (BT) and therefore eliminates the risk of crack initiation in the contact zone, in particular at the edge of the hole (BT). It is obvious that the compressive stress significantly reduced the crack initiation and hence increasing the lifetime of such bolted assembly, while the traction accelerates the risk of the initiation of fatigue crack. So it is necessary to identify the critical position in the contact surface which leads to the failure of the bolted assembly from the analysis of the stress

distribution at the interface between steel and aluminum plates (position 2) for which we observed the tension and compression in the contact area (position 2).

### 3.2.2 Distribution of Stress at Position 2

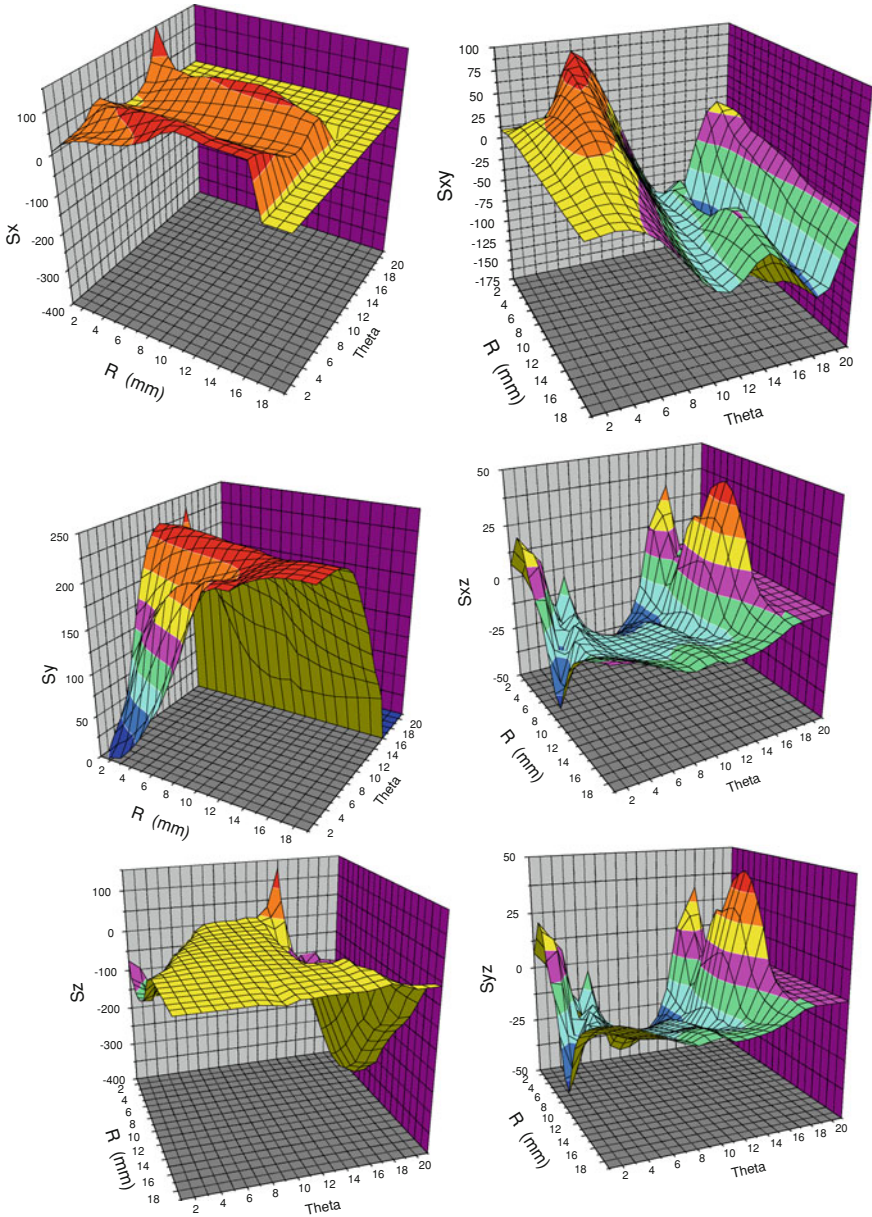
It is necessary to demonstrate the capacity of the finite element model to predict the characteristics of all the stresses at the interface in the contact surfaces for the bolted assembly. This information is not easily accessible from the experience especially in the interface between steel and aluminum plates (position 2). The numerical analysis is an alternative method to provide additional information for a better understanding for the case of bolted assemblies under fatigue. Figure 8 shows the evolution of each stress component in Cartesian coordinates at the contact zone characterized by the radius  $R$  and angle theta  $\theta$  (see Fig. 1) at the interface between steel and aluminum plates (position 2). Figure 8 shows that the stress which triggers the initiation and propagation of the crack in the edge of the contact area (BC) is important for those on the edge of the hole (BT) in particular positions characterized by the angle  $\theta$  less  $90^\circ$  ( $\theta < 90^\circ$ ) along the (BC). We also observe that the constraint ( $\sigma_z$ ) in the direction of tightening is higher at the edge of the hole (BT) compared to the contact edge (BC). This is usually due to the high pressure generated in the contact surfaces by the elements of assembly (screw-nut) during clamping phase. The interaction between the tightening torque and the level of cyclic loading will produce a friction phenomenon at the interface of the contact surfaces which leads to cracking or degradation of the contact surfaces under a fatigue stress. Therefore, the finite element model is considered effective to predict the failure of the bolted joint. It is interesting to trace the distribution of stress ( $\sigma_y$ ) in the direction of cyclic loading as a function of angle  $\theta$  in the contact area (position 2) for different radius ( $R$ ) in order to locate the point of crack initiation at the contact area.

Figure 9 illustrates the stress in the direction of cyclic loading ( $\sigma_y$ ) as a function of the angle  $\theta$  for three radius ( $R = 6.5, 8.0$  and  $12.5$  mm). According to this Fig. 9a, we can see that the curves had two well differentiated parts. Whatever the radius in the contact area is (position 2), all constraints are negative for orientation characterized by the angle  $\theta > 100^\circ$ , which means that there is lower risk of crack initiation in this portion at the contact surface. In positions between  $0^\circ \leq \theta \leq 43^\circ$ , the ( $\sigma_y$ ) stress increases gradually and finally reaches the maximum value for positions close to an orientation  $\theta = 43^\circ$  for each radius in the contact area. Beyond this position ( $\theta > 43^\circ$ ) the stress decreases to achieve the null value as function of the angle  $\theta$  and the radius ( $R$ ) in the contact area. We note that there is a critical stress value corresponds to an orientation of  $\theta = 43^\circ$  at the edge of the contact zone characterized by the radius ( $R = 12.5$  mm). We can therefore conclude that the initiation and the propagation of cracks in the interface between steel and aluminum plates (position 2) is in a favorable orientation characterized by the angle  $\theta = 43^\circ$  relative to the direction of cyclic loading. These results lead us to study the evolution of the stress according to the orientation ( $\theta = 43^\circ$ ) for different



**Fig. 7** The distribution of stress component along the BT and BC in contact zone (position 1)

radius in the contact zone and for a radius exceeding the limit of the contact area. Figure 9b shows the evolution of the stress ( $\sigma_y$ ) at  $\theta = 43^\circ$  as a function of radius  $R$ . We note that the stress ( $\sigma_y$ ) increases significantly with the radius. The maximum value is achieved for a radius  $R$  varied between 8.0 and 12.5 mm ( $8 \leq R \leq 12.5$ , where  $R = 12.5$  is the radius of the edge of the contact surface at the interface between steel-aluminum: position 2), after the stress decreases for a higher radius ( $R > 12.5$  mm: radius higher as the edge of the contact surface). So,



**Fig. 8** The distribution of stress component along the BT and BC in contact zone (position 2)

our calculation at the interface steel-aluminum (position 2) has been limited to a radius not exceeding a value of 12.5 mm ( $R \leq 12.5$  mm) although the size of the contact surface at the interface steel-aluminum (position 2) greatly exceeds the size seen in the numerical calculation.

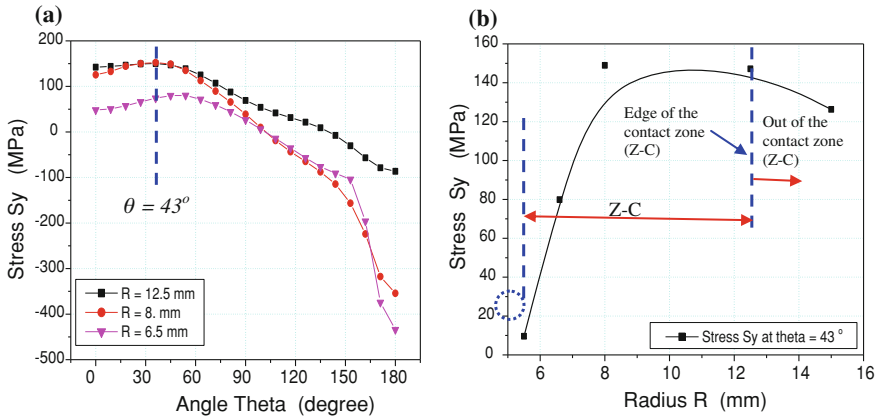


**Fig. 9** The distribution of stress  $\sigma_y$  : **a** in contact zone for various radius (position 2), **b** an contact zone for angle  $\theta = 45^\circ$  for various radius (position 2)

We can now say that the size of the contact surface between the two plates (position 2) is strongly influenced by the intensity of the torque. For radius far from the center of the bolt ( $R > 12.5$  mm) there is displacement with no friction in the contact surface. So, these surfaces at the interface of the plates are not in contact then no charge transfer occurs in these areas. For radius varied between 5.5 and 12.5 mm ( $5.5 \leq R \leq 12.5$ , where  $R = 5.5$  mm is the radius of the hole), there are now two different conditions: adhesion (stick) and sliding (slip) in different levels of cyclic loading.

### 3.2.3 Contact Status at Position 1

It has been observed through literature review [20, 21] that the fretting contact zone is divided into two zones: adhesion zone (stick) and a sliding zone (slip). The knowledge of these two areas in a contact problem is no longer possible with the option of contact STATUS in ANSYS software. In addition, we recall also that the cracking phenomenon of the fretting fatigue occurs in the transitional phase stick-slip which is considered as the most critical phase according by many authors [20–24]. Figure 10 illustrates the contact STATUS at the interface between the pad and aluminum plate (position 1).

A first observation from the reading of this figure (Fig. 10) is that there are three different zones: red zone, characterizes the adhesion (Stick) where you can not connect the friction stress as a function of pressure according to Coulomb’s law; orange zone, characterizes the slip where one can connect the friction stress as a function of pressure according to Coulomb’s law; yellow zone, characterizes the non-contact in position 1. A concentration of stress between the sticking and the sliding zones which leads to the risk of crack initiation within the contact zone

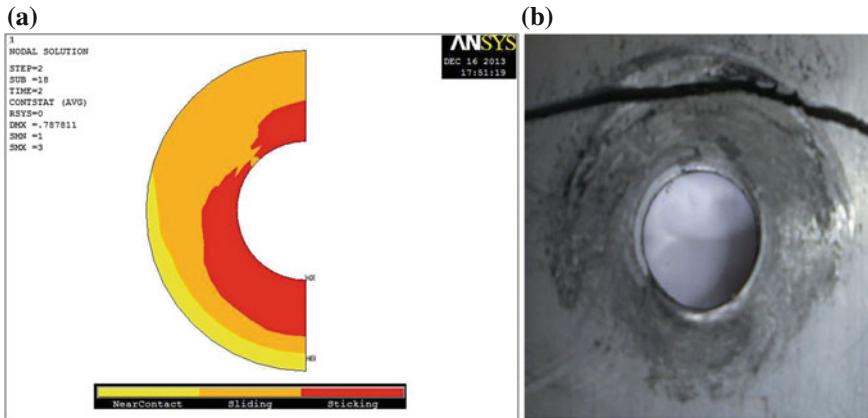


**Fig. 10** **a** Status of the contact area (position 1) and **b** the experimental observation ( $T = 6 \text{ daN.m}$  and  $F_{\text{max}} = 12 \text{ KN}$ )

(position 1) in favorable positions. In conclusion, a transition from the sticking contact to the sliding contact characterized by an angle  $\theta = 45^\circ$ .

To pinpoint the favorable orientation of the risk of crack initiation at the interface between the pad and aluminum plate (position 1), we present in Fig. 11 the evolution of the contact pressure, the friction stress and the sliding along the two paths (BT and BC) in the contact zone (position 1).

From Fig. 11, a first note is that the friction stress in positions characterized by the angle  $\theta$  above  $90^\circ$  is zero and for angles  $\theta \leq 90^\circ$ , the friction stress increases as function of angle  $\theta$  to reach their optimum value at angle  $\theta = 0^\circ$  along the contour B–C. The same trend is observed for the evolution of slip and contact pressure, where the slip takes the maximum value at  $\theta = 0^\circ$ . This indicates that the risk of crack initiation takes place in this portion in the zone of contact ( $\theta \leq 90^\circ$ ) during loading. We recall that the sliding at the edge of the hole (B-T) is negligible compared to the sliding at the edge of the contact zone (BC) due to the intensity of torque during the clamping phase.

### 3.2.4 Contact Status at Position 2

As previously mentioned, the torque and the level of cyclic loading have a significant effect on the distribution of contact STATUS (stick, slip and non-contact) in the contact zone, in particular at the interface between steel and aluminum plates (position 2).

Figure 12 presents the effect of the level of cyclic loading on the contact STATUS for a torque value equal to 8 Nm ( $T = 8 \text{ Nm}$ ). Three levels of cyclic loading are considered: 0 % of the cyclic loading (0 %  $F$ ) is only in the tightening phase, 100 % of the cyclic load (100 %  $F = F_{\text{max}}$ ) is the maximum value of the

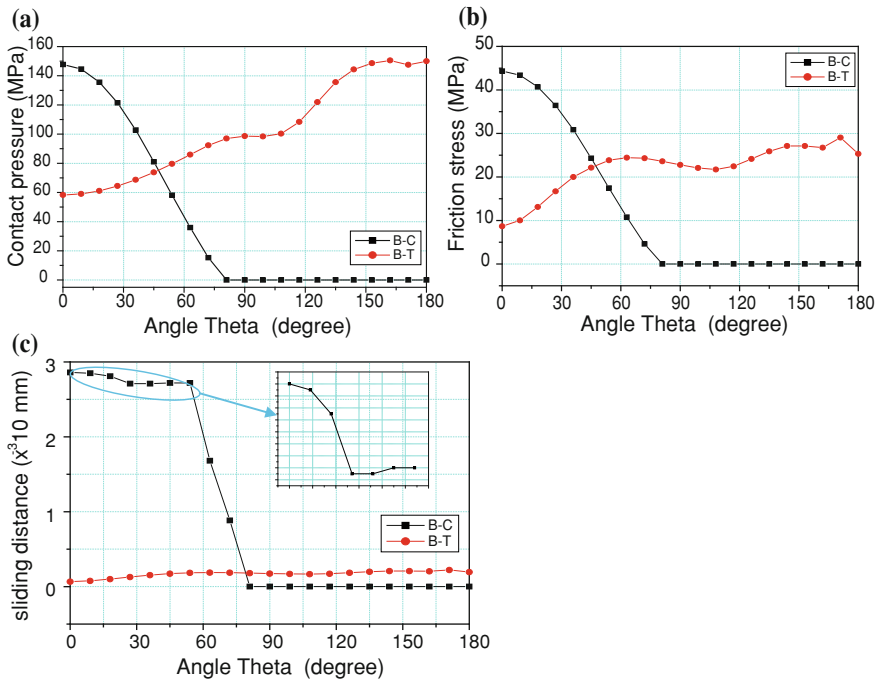


**Fig. 11** The distribution of **a** contact pressure, **b** friction stress and **c** the sliding along the BT and BC in contact zone (position 1)

cyclic load and 50 % of  $F_{max}$  corresponding to an average load ( $0 \% F_{max} < F < 100 \% F_{max}$ ). The analysis of Fig. 12 shows that, whatever the level of cyclic loading for this level of torque, the stick (adhesion) and slip zones were observed for a radius less than 12.5 mm ( $R \leq 12.5$  mm) in the contact zone (position 2). For a radius greater than 12.5 mm ( $R > 12.5$  mm), there is no-contact at the interface between steel and aluminum plates. So, the adhesion and slip zones completely disappear for  $R > 12.5$  mm. We also see in this contact zone ( $R \leq 12.5$  mm) that the adhesion zone decreased with increasing of the level of cyclic loading and her size decreases on 50 % of the maximum cyclic loading ( $50 \% F_{max}$ ). So, the transition from sticking (adhesion) to sliding is the most critical phase in fretting fatigue. Generally, the cracking occurs in this area.

One of the most important parameters which control the fretting fatigue life of bolted assembly is the sliding at the interface of the contact surfaces (position 2). Knowledge of the slip distribution is fundamental in the contact area in order to locate precisely the site of crack initiation at the interface between steel and aluminum plates (position 2). Figure 13 shows the distribution of slip for this loading condition. From Fig. 13 we observe that the value of the slip is even more important when approaching to the border of the contact zone ( $R \rightarrow 12.5$ ), particularly in positions characterized by the angle  $\theta$  less of  $50^\circ$  ( $\theta < 50^\circ$ ) along the

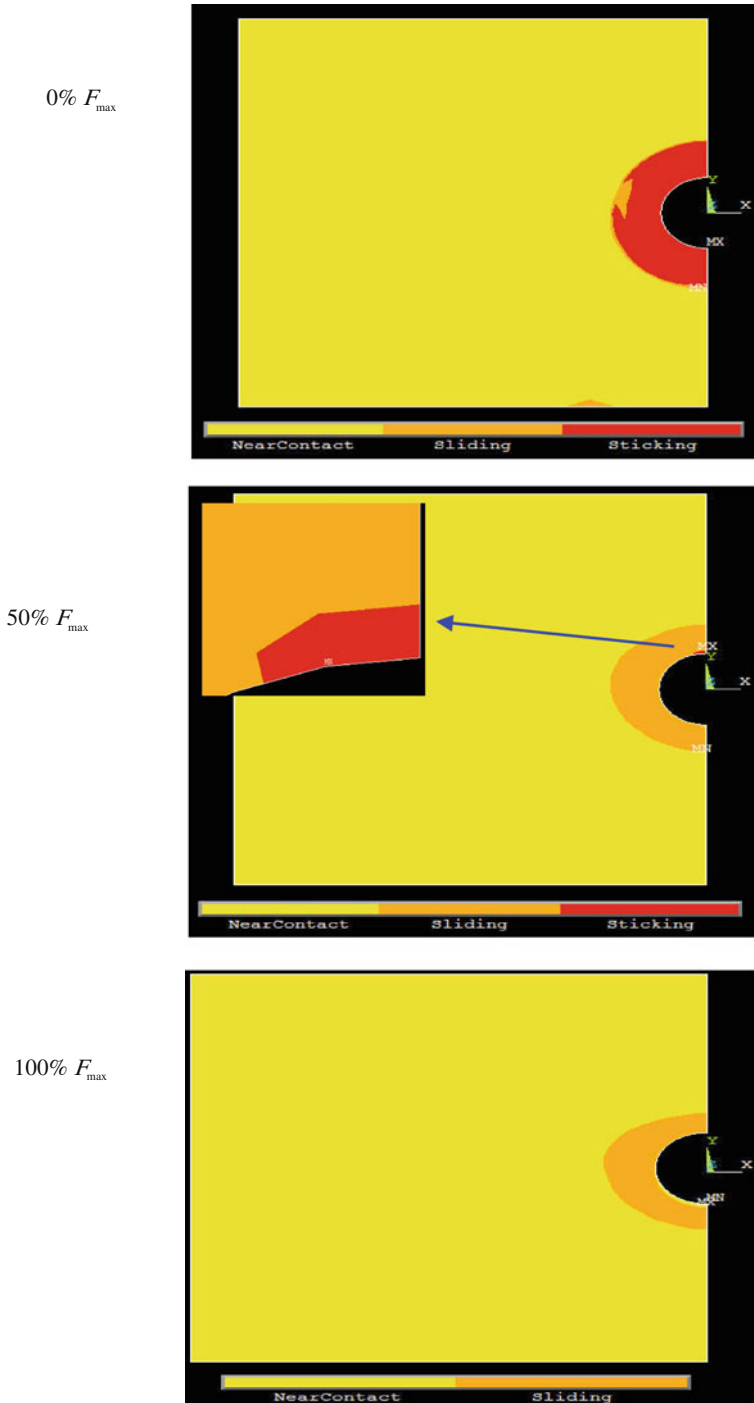
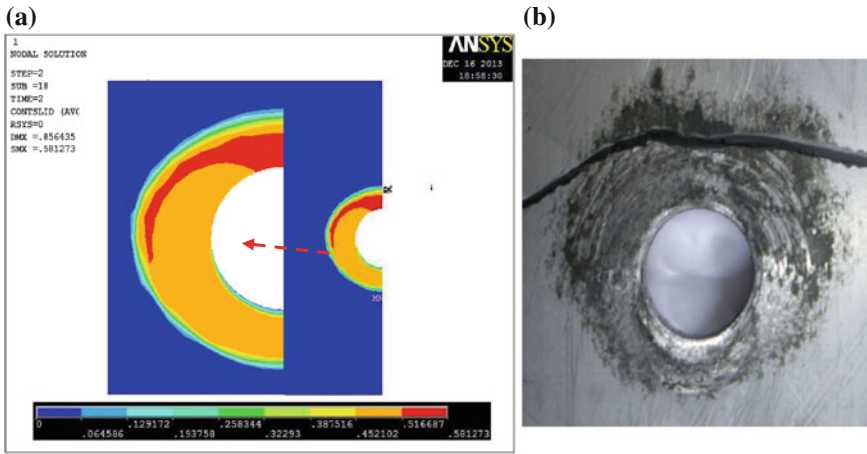


Fig. 12 Status of the contact area (position 2) versus to the cyclic loading for  $T = 6$  daN.m





**Fig. 13** **a** The distribution of sliding in the contact area (position 2) and **b** the experimental observation ( $T = 6$  daN.m and  $F_{max} = 12$  KN)

edge of the contact zone (BC). Therefore, through all the numerical results and experimental observations [2] we can now consider that the risk of crack initiation of any bolted assembly occurs in the edge of the contact zone (BC) in orientation inclined at an angle  $\theta$  varied between 40 and 50° ( $40^\circ \leq \theta \leq 50^\circ$ ) relative to the direction of cyclic loading. The comparison between the experimental results and the status of the contact (Fig. 10b) leads to the same conclusion.

### 4 Conclusions

The aim of this study was to analyze the effect of tightening torque on bolted assemblies under fretting fatigue condition. From these experimental and numerical results, we can deduce the following conclusions:

- The developed finite element modelling approach to simulate clamping force (tightening torque) in the bolt of such bolted assembly was validated against the experimental results.
- The size of the adhesion and slip zones in the contact zone is related at the magnitude of tightening torque.
- Crack initiation changes from the edge of the hole to close the edge of contact zone.
- The magnitude of the clamping torque and the level of cyclic loading determine the mode failure of bolted assemblies.
- The crack initiation will be transferred to the edge of the contact zone at the interface between steel and aluminium plates (position 2) in a plane inclined at an angle  $\theta$  varied between 40 and 50° relative to the sliding direction.

## References

1. Guo, R., Duan, R.C., Mesmacque, G., et al.: Fretting fatigue behavior of riveted Al6XXX components. *Mater. Sci. Eng. A* **483–484**, 398–401 (2008)
2. Benhamena, A., Talha, A., Benseddig, N., et al.: Effect of clamping force on fretting fatigue behaviour of bolted assemblies: Case of couple steel–aluminium. *Mater. Sci. Eng. A* **527**, 6413–6421 (2010)
3. Iyer, K., Hu, S.J., Brittman, F.L., et al.: Fatigue of single-and double-rivet self-piercing riveted lap joints. *Fatigue. Fract. Eng. Mater. Struct.* **28**, 997–1007 (2005)
4. Chen, Y.K., Han, L., Chrysanthou, A., et al.: Fretting wear in self-piercing riveted aluminium alloy sheet. *Wear* **255**, 1463–1470 (2003)
5. Han, L., Chrysanthou, A., Young, K.W., et al.: Characterization of fretting fatigue in self-piercing riveted aluminium alloy sheets. *Fatigue. Fract. Eng. Mater. Struct.* **29**, 646–654 (2006)
6. Valtinat, G., Hadrych, I., Huhn, H.: Strengthening of riveted and bolted steel constructions under fatigue loading by preloaded fasteners—experimental and theoretical investigations. In: *Proceedings of the International Conference on Connections in Steel Structures IV*, AISC and ECCS, Roanoke, USA (2000)
7. Lee, H., Mall, S.: Fretting behavior of shot peened Ti-6Al-4V under slip controlled mode. *Wear* **260**, 642–651 (2005)
8. Lee, H., Mall, S.: Investigation into effects and interaction of various fretting fatigue variables under slip-controlled mode. *Tribol. Int* **39**, 1213–1219 (2006)
9. Hutsona, A., Lee, H., Mall, S.: Effect of dissimilar metals on fretting fatigue behavior of Ti-6Al-4V. *Tribol. Int* **39**, 1187–1196 (2006)
10. Rajasekaran, R., Nowell, D.: Fretting fatigue in dovetail blade roots: experiment and analysis. *Tribol. Int* **39**, 1277–1285 (2006)
11. Sadeler, R.: Influence of contact pressure on fretting fatigue behaviour of AA 2014 alloy with dissimilar mating material. *Fatigue. Fract. Eng. Mater. Struct.* **29**, 1039–1044 (2006)
12. Xu, J.Q., Mutoh, Y.: Stress field near the contact edge in fretting fatigue tests. *JSME Int. J. Ser. A* **45–4**, 510–516 (2002)
13. Wright, G.P., O’Conner, J.J.: Finite-Element Analysis of alternating axial loading of an elastic plate between two elastic rectangular blocks with finite friction. *Int. J. Eng. Sci.* **9**, 555–570 (1971)
14. Nagata, K., Fukakura, J.: Effect of contact materials on fretting fatigue strength of 3.5Ni-Cr-Mo-V rotor steel and life prediction method. *Trans. Jpn. Soc. Mech. Eng.* **58–553**, 1561–1568 (1992)
15. Jayaprakash, M., Mutoh, Y., Asai, K., et al.: Effect of contact pad rigidity on fretting fatigue behavior of NiCrMoV turbine steel. *Int. J. Fatigue.* **32**, 1788–1794 (2010)
16. Chakherlou, T.N., Shakouri, M., Akbari, A., et al.: Effect of cold expansion and bolt clamping on fretting fatigue behaviour of Al 2024-T3 in double shear lap joints. *Eng. Fail. Anal.* **25**, 29–41 (2012)
17. Hills, D.A., Nowell, D.: *Mechanics of fretting fatigue*. Kluwer Academic Publishers, Dordrecht (1994)
18. Swanson Analysis Systems Inc. ANSYS, User’s guide for revision11, ANSYS 11 Documentation, ANSYS Element reference, Element, library. SOLID45/CONTA173 (2007)
19. Wagle, S., Kato, H.: Ultrasonic detection of fretting fatigue damage at bolt joints of aluminium alloy plates. *Int. J. Fatigue.* **31**, 1378–1385 (2009)
20. Cattaneo, C.: Sul Contato di Due Corpo Elastici, *Accademia dei Lincei, Rendiconti, Series 6–27*:342–348, 434–436 and 474–478 (1938)
21. Mindlin, R.D.: Compliance of elastic bodies in contact. *J. Appl. Mech. Trans. ASME* **16**, 259–268 (1949)
22. Waterhouse, R.B.: *Fretting fatigue*. Applied Science Publishers, London (1981)
23. Vingsbo, O., Soderber, S.: On fretting maps. *Wear* **126**, 131–147 (1988)
24. Munoz, S., Proudhon, H., Dominguez, J., et al.: Prediction of the crack extension under fretting wear loading conditions. *Int. J. Fatigue.* **28**, 1769–1779 (2006)